REMOTE SENS. ENVIRON. 35:105–119 (1991)

Vegetation Indices in Crop Assessments

C. L. Wiegand, A. J. Richardson, D. E. Escobar, and A. H. Gerbermann

Remote Sensing Research Unit,
USDA Agricultural Research Service, Weslaco, Texas

Vegetation indices (VI), such as greenness (GVI), perpendicular (PVI), transformed soil adjusted (TSAVI), and normalized difference (NDVI), measure the photosynthetic size of plant canopies and portend yields. A set of equations, called spectral components analysis (SCA), that interrelates VI or cumulative seasonal VI (ΣVI), leaf area index (L), fractional photosynthetically active radiation (FPAR, dimensionless), cumulative daily PAR energy absorbed (ΣAPAR, MJ/m²), above-ground dry photomass (DM, g/m²), and economic yield (Y, g/m²) are presented and used to analyze data from two studies conducted in 1989. In one study we made boll counts and percent plant cover measurements in a salt-affected cotton field on 60 m grid intervals and calculated GVI, PVI, TSAVI, and NDVI at the grid intersections for SPOT-1 HRV and videography scenes. The four VI from SPOT accounted for more of the variation in the lint yield estimated from the boll counts (75–76%) than those from videography (61–63%), but VI from the different systems each accounted for 67% of the variation in plant cover. All relations were linear. In the other study, reflectance factors and FPAR were measured periodically during the season in corn planted at three densities (7.7, 5.4, and 3.1 plants/m²). FPAR could be estimated from NDVI and PVI, respectively, by FPAR = −0.344 + 0.229exp(1.95 NDVI) ($r^2 = 0.973$) and FPAR = 0.015 + 0.036(PVI) ($r^2 = 0.956$). Methods of obtaining FPAR and their effect on the efficiency of conversion of APAR to DM are illustrated and discussed. The data demonstrate how SCA unifies and strengthens the scientific basis of VI interpretations.

INTRODUCTION

Various spectral vegetation indices (Rouse et al., 1973; Kauth and Thomas, 1976; Richardson and Wiegand, 1977; Tucker et al., 1979; Perry and Lautenschlager, 1984) have been developed that reduce multiband observations to a single numerical index. The index is typically a sum, difference, ratio, or other linear combination of reflectance factor or radiance observations from two or more wavelength intervals. High absorption of incident sunlight in the visible red (RED, 600–700 nm) portion and strong reflectance in the near-infrared (NIR, 750–1350 nm) portion of the electromag-

Address correspondence to C. L. Wiegand, Remote Sensing Research Unit, USDA/ARS, 2413 E. Highway 83, Weslaco, TX 78596-8344.

Received June 1990; revised 12 November 1990.

0034-4257/91/$3.50

655 Avenue of the Americas, New York, NY 10010

netic spectrum by photosynthetically active tissue in plants is distinctive from that of soil and water, the other two predominant landscape features. Thus, vegetation indices developed from spectral observations in these two wavelengths have correlated highly with the plant stand parameters green leaf area index (L), chlorophyll content, fresh and dry above-ground phytomass (FM, DM), plant height, percent ground cover by vegetation, plant population, and grain or forage yield (Rouse et al., 1973; Wiegand et al., 1973; Richardson et al., 1974; Pearson et al., 1976; Thomas and Gausman, 1977; Tucker, 1977; Wiegand et al., 1979; Curran, 1980; Holben et al., 1980; Kimes et al., 1981; Aase and Siddoway, 1981; Walburg et al., 1982; Richardson et al., 1982; and many others subsequently).

More specifically, vegetation indices have been considered a measure of vegetation density or cover (Wiegand et al., 1973); photosynthetically active biomass (Tucker, 1979; Wiegand and Richardson, 1984); leaf area index (Wiegand et al., 1979); green leaf density (Tucker et al., 1985); photosynthesis rate (Sellers, 1985; 1987); amount of photosynthetically active tissue (Wiegand et al., 1986b; Wiegand and Richardson, 1987); and photosynthetic size of canopies (Wiegand et al., 1989; Wiegand and Richardson, 1990).

The cited empirical studies have been complemented by modeling efforts. Goel (1988) has summarized the essence of a large number of canopy bidirectional reflectance models among which SAIL (Verhoef, 1984) is the most widely used, and described their inversion to estimate canopy biophysical variables. Sellers (1985; 1987) has presented theoretical arguments and used a two-steam radiative transfer model to show how vegetation indices relate to canopy resistance and rate of photosynthesis. Goel and Thompson (1984) developed a general technique for the sensitivity analysis of canopy reflectance models and Choudhury (1987) examined the relationships among vegetation indices, FPAR, and net photosynthesis using sensitivity analysis.

Questions remain, however, about the interpretation of vegetation indices in terms of the current condition and likely productivity of crop, range, and forest plant communities. The purpose of this paper is to provide examples from studies conducted in 1989 of the relation between vegetation indices and crop performance and to discuss them in terms of agronomic and plant physiological principles embodied in spectral components analysis (SCA) (Wiegand and Richardson, 1984; 1987; 1990; Wiegand et al., 1989).

METHODS

Field Measurements

Cotton

A salt-affected field of cotton (*Gossypium hirsutum* L.) 15 km NE of Weslaco, Texas, that measured 388 m across and had rows oriented E–W 384 m long spaced 1.02 m apart (14.9 ha actual planted area) was selected after the crop was established. The soil in the field ranged from nonsaline to so saline that plants did not emerge. The pattern and severity was very irregular (Plate I) as is typical of this stress (Carter and Wiegand, 1965). A square grid of 36 sample sites at 60 m intervals was positioned within the field so that no site was within 30 m of the field boundary.

SPOT-1 HRV data (wavelengths: green (GR), 500–590 nm; (RED), 610–680 nm; NIR, 790–890 nm) were acquired on 4 June 1989 from 13° east, while narrow band multispectral videography (wavelengths: yellow–green (YG), 543–552 nm; RED, 644–656 nm; and NIR, 815–827 nm) using the high resolution multispectral video system described by Everitt et al. (1991) was obtained on 19 June and 14 July 1989 from 1400 m altitude. Plant height (PH, m) and percent plant cover (PC) were measured on 5 July on average sized plants within 10 m of the grid intersections. Plant height measurements were made looking horizontally across the tops of plants to a meter stick and plant cover was determined from measured width of plants in the row divided by row spacing times 100. The number of bolls large enough to mature were counted on 2 m of row (2.04 m^2) near the grid intersection on 12 and 13 July. Boll counts were converted to kg lint/ha based on 600 bolls/kg lint (L. N. Namken, personal communication) and expanded from the size of the sample to hectares.

Corn

The corn (*Zea mays* L.) experiment, conducted at the ARS North Farm, Weslaco, Texas (26.2°N, 98.0°W), consisted of three populations (7.7, 5.4, and 3.1 plants/m^2) of field corn, cultivar Conlee

202, replicated 6 times in plots of 8 rows spaced 0.75 m apart and 15.2 m long. The crop was planted on 13 March and emerged on 18 March. It reached the 10-leaf stage on 19 April and began tasseling 8 May. The various plots reached the silk stage between 14 May and 19 May, and physiological maturity of the grain, as indicated by black layer formation, from 23 to 30 June.

Plots that had reached physiological maturity by then were harvested 28 June and the remainder on 1 July. Harvest consisted of cutting all plants off just above the ground in 1 m^2 areas (1.33 m long row segments) in each plot, removing and putting the husked ears in one bag and all other harvested plant material in another. After about 2 weeks of drying in an unventilated, uncooled glass greenhouse, the grain was shelled from the ears and the cobs were added to the other stover. The grain yield (g/m^2) consisted of the shelled grain that averaged 5.4% moisture while the grain plus all the other aboveground plant parts constituted the dry phytomass (DM, g/m^2).

The experimental area was fertilized twice with liquid nitrogen at the rate of 55 kg/ha, once on 28 March and again on 17 April. The experimental area was irrigated prior to planting and on 4 April, 10 May, and 7 June.

Spectral radiance measurements were taken near solar noon from 2.8 m above the ground using a Mark II radiometer (Tucker et al., 1981) mounted on an aluminum pole on 11 dates beginning on 31 March and ending 26 June. The spectral bands of the Mark II are 630–690 nm and 760–900 nm and its field of view was 15°. Two observations per plot were taken centered over the corn row and two centered over the furrow (each at different places) and the measurements were averaged. Each end of approximately a 2 m long segment on the third row in from the north side of the plots was flagged and we returned to this row segment for all Mark II measurements.

Photosynthetically active radiation (PAR) incident on (I_0), transmitted through (T), reflected from the composite canopy–soil backgrounds (R), and reflected from the bare soil (R_s) provided the data for fractional absorbed PAR (FPAR) defined (Hipps and Kanemasu, 1983; Gallo et al., 1985) as

$$\text{FPAR} = (I_0 - T - R + TR_s)/I_0. \qquad (1)$$

LI-COR[1] line quantum sensors (LI-191SB) were used to measure T, R, and R_s, and I_0 was measured using a quantum sensor (LI-190SB).[1] For the T measurements the line quantum sensor (LQS) was inserted below the canopies obliquely middle-to-middle. For measurements of R (canopy plus soil) the LQS was inverted 0.3 m above the canopies and parallel to the sensor below the canopies. The R_s term was measured by an LQS inverted 0.3 m above a small area in the plots where the plants had been removed soon after emergence and weeds were controlled by hoeing frequently. The T and R sensors were moved to new canopy sites for each of four measurements in each plot. The quantum sensor was mounted on a 2-m-tall stand that was moved from plot to plot and leveled at each stop. Sensors had been intercalibrated before the season began. The sensor outputs for T, R, and I_0 and the time of observations were electronically logged simultaneously. Care was taken to keep all sensors level and to avoid shading the sensor measuring T by the one measuring R. The PAR measurements described were made on seven dates beginning 29 March and ending 16 June. These measurements were also made on the third row from the north in each plot but at sites different from the reflectance factor observations to avoid trampling.

Data Preprocessing

SPOT. Digital counts for a 51×81 pixel area surrounding the test cotton field were extracted from the SPOT scene digital tapes using a PCI EASI/PACE 512×512 image analysis system interfaced to a COMPAQ 386/25 microcomputer. Line printer listings were generated, the boundaries of the test and surrounding fields were identified in these "gray maps," and the pixels closest to the grid intersections were manually selected using the pattern of plant growth visible in the gray maps and reference aerial photographs as guides.

Reflectance at the top of the atmosphere (Rt_i) was computed from the equation (Moran et al.,

[1]Mention of trade names does not infer preferential treatment nor endorsement by the U. S. Department of Agriculture over similar products available from other sources.

1990)

$$Rt_i = [\pi(DC_i / c_i)d^2] / [Es_i(\cos SZA)], \quad (2)$$

wherein c_i are gain-dependent calibration coefficients for each band (*SPOT Data User's Handbook*, Fig. 3-11) that convert digital counts (DC_i) to radiance at the sensor (gains for determining C_i were 6, 7 and 5 for HRV bands 1, 2 and 3, respectively), d is the earth/sun distance in astronautical units, Es_i is the exoatmospheric solar irradiance ($W m^{-2} sr^{-1} \mu m^{-1}$) in band i, and SZA is the solar zenith angle at the time the scene was acquired. For the 4 June scene the factors that converted digital counts to reflectance were 0.182, 0.221, and 0.347 for bands 1, 2, and 3, respectively. We used the reflectance at the top of the atmosphere to represent ground level conditions. Bare soil areas in the 4131 pixel subscene provided data for determining the soil line.

Multispectral Videography

Data from each camera of the airborne video system (Everitt et al., 1991) were recorded on $\frac{1}{2}$-in. format Super VHS Panasonic Model AG-7400 portable video cassette recorders. The black-and-white cameras (COHU Model 4810 series) were equipped with synchronized generator lock connections so that continuously synchronized composite imagery and its black-and-white components were acquired.

A Matrox MVP digitizing board and IMAGER software were used to digitize the individual bands' scenes for storage on the hard disk of a microcomputer interfaced to an ERDAS image analysis system. ERDAS software was used to position polygons 7 pixels × 7 pixels in size centered on the grid intersections, extract the digital counts, and determine their means and standard deviations. The procedures were speeded by registering all bands to the NIR band on one date, so that pixel samples could be extracted from the individual bands on both dates by one set of polygon coordinates. Samples of bare soil areas (turn rows, field roads, and barren sites in fields) within the video scenes were used to determine the soil line (Table 1).

Mark II

The Mark II data were processed to reflectance factors using the procedures described by Richardson (1981). Currently, a halon panel is used as the reference standard and white-painted plywood as working panels. The same small areas where the bare soil PAR reflectance (R_s) term was measured were used each measurement date to obtain the reflectance factors of wet and dry soil from a height of 1–1.2 m. Water from a sprinkler can was applied to wet an approximately 0.7 m^2 area. The periodically obtained wet and dry soil reflectance factors were pooled to determine a soil line for the entire season.

Table 1. Soil Line (SL) and Vegetation Index Equations by Sensor System and Crop

Sensor System	*Scene*	*Equations*
A. Cotton		
SPOT HRV-1	4 June	SL: RED = −8.20 + 1.099 NIR
		GVI = 0.841 NIR − 0.438 RED − 0.317 GR − 5.84
		PVI = 0.740 NIR − 0.673 RED − 5.52
		TSAVI = 0.910 (NIR − .910 RED − 7.46)/(RED + 0.91 NIR − 6.79)
Video	19 June	SL: RED = 1.50 + 1.032 NIR
		GVI = 0.837 NIR − 0.401 RED − 0.372 YG − 2.69
		PVI = 0.718 NIR − 0.696 RED + 1.04
	17 July	SL: RED = −15.5 + 1.265 NIR
		GVI = 0.863 NIR − 0.451 RED − 0.228 YG − 14.89
		PVI = 0.784 NIR − 0.620 RED − 9.61
B. Corn		
Mark II	Periodic	SL: RED = −2.01 + 0.765 (NIR)
		PVI = 0.608 RIR − 0.794 RED − 1.60
All		NDVI = (NIR − RED)/(NIR + RED)

Vegetation Indices

The three-band greenness vegetation index (GVI) was determined for both SPOT-1 HRV and three-band video data using the n-space procedure of Jackson (1983) with one modification: We calculated the greenness of the soil plane using the coefficients from the n-space procedure and added it algebraically to the greenness equation. This modification permits the soil plane to have a non-zero intercept and a greenness of zero.

Since the perpendicular vegetation index (PVI) (Richardson and Wiegand, 1977) is the orthogonal distance from a vegetation point in NIR and RED, or NIR and GR, 2-space, we used the equation for a perpendicular to a line (Jackson et al., 1980), instead of the original formula, to calculate it. For NIR on the abscissa and RED on the ordinate the equation is

$$\mathrm{PVI}_{\mathrm{NIR,RED}} = [a_1(\mathrm{NIR}) - \mathrm{RED} + a_0] / [1 + (a_1)^2]^{1/2}, \quad (3a)$$

where a_0 is the soil line intercept and a_1 is the slope of the soil line. When the soil line is presented with NIR on the ordinate and RED on the abscissa, the equation is

$$\mathrm{PVI}_{\mathrm{RED,NIR}} = [\mathrm{NIR} - a_1(\mathrm{RED}) - a_0] / [1 + (-a_1)^2]^{1/2}, \quad (3b)$$

where a_0 and a_1 are, again, the intercept and slope of the soil line. In this study the soil line was determined by least squares (Mark II data) or graphically (SPOT and video data). The transformed soil adjusted vegetation index, $\mathrm{TSAVI}_{\mathrm{RED,\,NIR}}$ (Baret et al., 1989), is defined by

$$\mathrm{TSAVI}_{\mathrm{RED,NIR}} = a_1[\mathrm{NIR} - a_1(\mathrm{RED}) - a_0] / [\mathrm{RED} + a_1(\mathrm{NIR}) - a_1 \cdot a_0]. \quad (4)$$

Conceptually, TSAVI is a measure of the angle between the soil line and the line joining the vegetation point with the soil line intercept. For the special case of a soil line slope = 1.0 and intercept = 0, TSAVI reduces to NDVI defined by

$$\mathrm{NDVI} = (\mathrm{NIR} - \mathrm{RED})/(\mathrm{NIR} + \mathrm{RED}). \quad (5)$$

The specific equations of the soil lines and vegetation indices for the various data sets of this study are summarized in Table 1. The vegetation indices in Table 1 for SPOT data are calculated from exoatmospheric reflectances (%), from eight-bit digital counts (DC) for the video data, and from reflectance factors (%) for the Mark II data. The soil line equations are poor for the video data because the small areas in the scenes usually contained only dry soil that represented only a short segment of the soil line. Consequently, there was uncertainty in them. The built-in automatic gain control in the video cameras also made the DC of the soil unique for each overflight, so that data could not be pooled across dates.

Data Interpretation

One spectral components analysis equation (Wiegand and Richardson, 1984) is

$$\mathrm{FPAR(VI)} = \mathrm{FPAR}(L) \times L(\mathrm{VI}) = \mathrm{FPAR}(L[\mathrm{VI}]), \quad (6)$$

which is read as FPAR as a function of any vegetation index (VI) dominated by the NIR reflectance of the canopy equals FPAR as a function of leaf area index (L) times L as a function of VI. The equation states that because there is a functional relation between FPAR and L and between L and VI it follows that there is also one between FPAR and VI. Calibration of FPAR directly in terms of VI avoids the tedious labor of determining L, but, more importantly, makes FPAR estimates available for many remotely observable fields. It is now recognized that FPAR is a nearly linear function of VI and attempts at the biophysical explanation of the linearity have been made (Sellers, 1985; 1987; Choudhury, 1987).

An equation that contains the L(VI) term of Eq. (5) and incorporates economic yield (Y) is

$$Y(\mathrm{VI}) = L(\mathrm{VI}) \times Y(\mathrm{L}) = Y(L[\mathrm{VI}]), \quad (7)$$

where Y is the salable plant part as appropriate for the crop (grain, root, fruit, fiber, or above-ground biomass) (g/m^2). Equation (7) relates the photosynthetic capacity of the crop characterized by L and VI to its economic yield. The term L(VI) links Eqs. (6) and (7).

Measurements of VI made too early in the growing season or too late into senescence do not relate well to yield in Eq. (7) because the measurements do not represent the canopies' photosynthetic size. The values of VI corresponding to the plateau L values for the season, or the maximum leaf area index, L_m, observed for each field or treatment of interest, can be used to determine

the Y(VI) functional relation. As a rule, when L reaches its plateau value for the season, the sinks for photosynthetic assimilates are dominated by the plant parts that constitute yield.

An equation that expresses the left sides of Eqs. (6) and (7) as daily incremented cumulations, designated by Σ, and couples them through growth analysis (Warren Wilson, 1981) is

$$Y(\Sigma VI) = \Sigma APAR(\Sigma VI) \times \Delta DM(\Sigma APAR) \times Y(\Delta DM) \quad (8)$$

wherein

$$APAR = FPAR \times I_0. \quad (9)$$

Equation (8) provides the rationale for expecting yields (Y) to be estimable from cumulative daily vegetation indices, that is, from the area under the seasonal VI versus time curves. In Eq. (8), APAR is the product of daily FPAR (unitless) from Eq. (6) and daily incident PAR flux, I_0(MJ/m^2/day), which in cumulations has the units MJ/m^2. By its very nature DM is integral growth that we express as the dry matter change, ΔDM.

The cumulations of all terms of Eq. (8) begin logically at seedling emergence so that the cumulations for all variables begin either at zero or the value for bare soil. At seedling emergence DM_1 is so small that it is usually ignored. If economic yield (Y) of nonforage crops is of prime interest, ending date DM, DM_2, corresponds to either physiological maturity or to harvest, forcing all other terms to be evaluated at this end time.

Since FPAR can be estimated almost as well from VI as from L (Gallo et al., 1985; Wiegand and Richardson, 1987), ΣAPAR and ΣVI must also be closely related because APAR is the energy available for photosynthesis and VI is a measure of the photosynthetic size of canopy. We can anticipate that ΣVI will relate functionally to and provide a good estimate of yield if ΣAPAR would. We have termed the slope of the ΣAPAR(ΣVI) relation the efficiency of absorption (e_a, MJ m^{-2}/VI unit) in terms of the photosynthetic size of the canopy.

The second right side term, ΔDM(ΣAPAR), is often approximately linear for much of the season for a given planting (Monteith, 1977) and its slope is the efficiency of conversion of photosynthetically active radiation to dry mass (e_c, g DM/MJ), sometimes called radiation use efficiency (RUE). Under low to moderate stress conditions ΔDM(ΣAPAR) is linear because any reduction in APAR reduces the supply of assimilates of photosynthesis and consequently decreases the dry matter change (growth) proportionally.

When the full growing season, emergence to harvest, is considered the third term in Eq. (8), Y(DM_2), is, by definition, the harvest index. The harvest index is approximately 0.5 for starchy endosperm grain crops (e.g., corn, temperate cereals, grain sorghum) when adapted cultivars and recommended agronomic practices are followed unless extreme stress truncates reproduction (foliar disease, drought, for example). Evidence is accumulating (e.g., Howell, 1990) that the harvest index is climate-dependent, hence site-dependent.

The right-hand side terms in Eq. (8) do not need to be known or observed to use the left-hand side in applying remote observation capability; the right-hand side terms provide the agronomic and physiological explanation of why the left side relation exists and is meaningful. We have termed the slope of the Y(ΣVI) relation the yield efficiency (e_y, g m^{-2}/VI unit) in terms of the photosynthetic size of the canopy (Wiegand et al., 1989; Wiegand and Richardson, 1990). The numerical value of e_y is similar for the indices GVI and PVI, and for NDVI and TSAVI because those VI pairs have similar magnitudes.

Equations (6) and (7) described LANDSAT MSS observations for grain sorghum (*Sorghum bicolor* L. Moench) (Wiegand and Richardson, 1984) and small plot handheld radiometer studies for wheat (*Triticum aestivum* L.), cotton, and corn (Wiegand et al., 1986a, Wiegand and Richardson, 1987). Equations (6), (7), and (8) have been verified for rice (*Oryza sativa* L.) (Wiegand et al., 1989).

Spectral components analysis (SCA) assumes implicitly that i) plant stands integrate the growing conditions experienced and express the net assimilation through the canopies achieved, ii) stresses severe enough to affect economic yield will be detectable through their effects on the development and persistence of photosynthetically active tissue in the canopies, iii) high economic yields cannot be achieved unless plant canopies are achieved that fully utilize available solar radiation as the plants enter the reproductive stage, and iv) vegetation indices calculated from remote observations in appropriate wavelengths effectively

measure the photosynthetic size of the canopies. Equations (6), (7), and (8) are used to aid the interpretation of data from the studies reported herein.

RESULTS

Cotton

Figure 1 displays the scatter in the boll counts, expressed as lint yield (kg/ha), for the 36 samples from within the salt-affected cotton field versus the four vegetation indices calculated for the SPOT-1 HRV data. The functional relations are those for the left-hand side of Eq. (7) applicable to interpreting spectral data obtained during active reproduction by the crop. At the study site, cotton is blooming and setting bolls by 15 May. After 1 June the photosynthetic size of the canopy increases only modestly because assimilates in excess of those for respiration, water and nutrient uptake, and structural enlargement support boll growth, which continues for individual bolls for about 40 days. Consequently, the photosynthetic

Figure 1. Lint yield of cotton versus four vegetation indices calculated from SPOT-1 HRV observations.

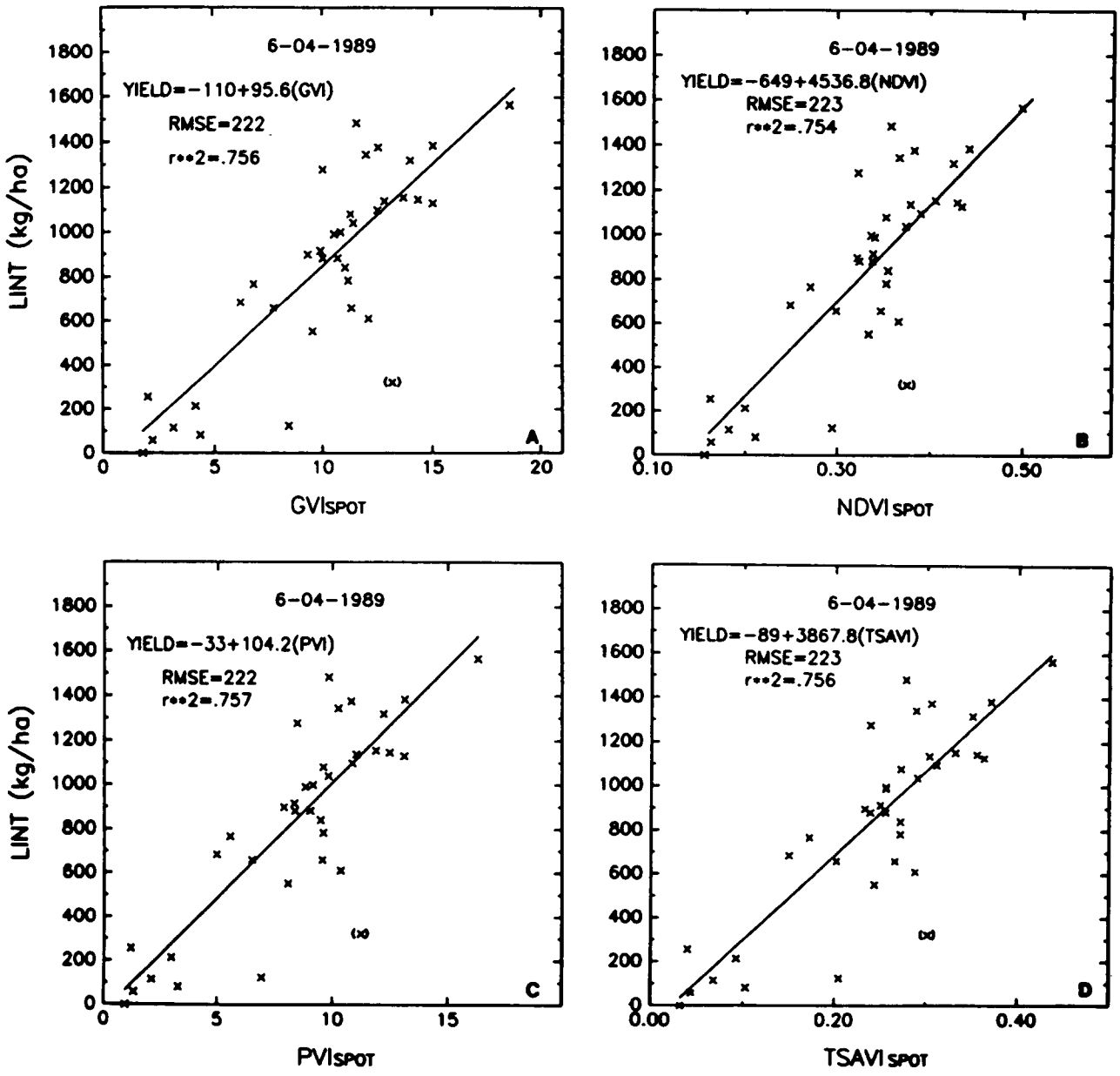

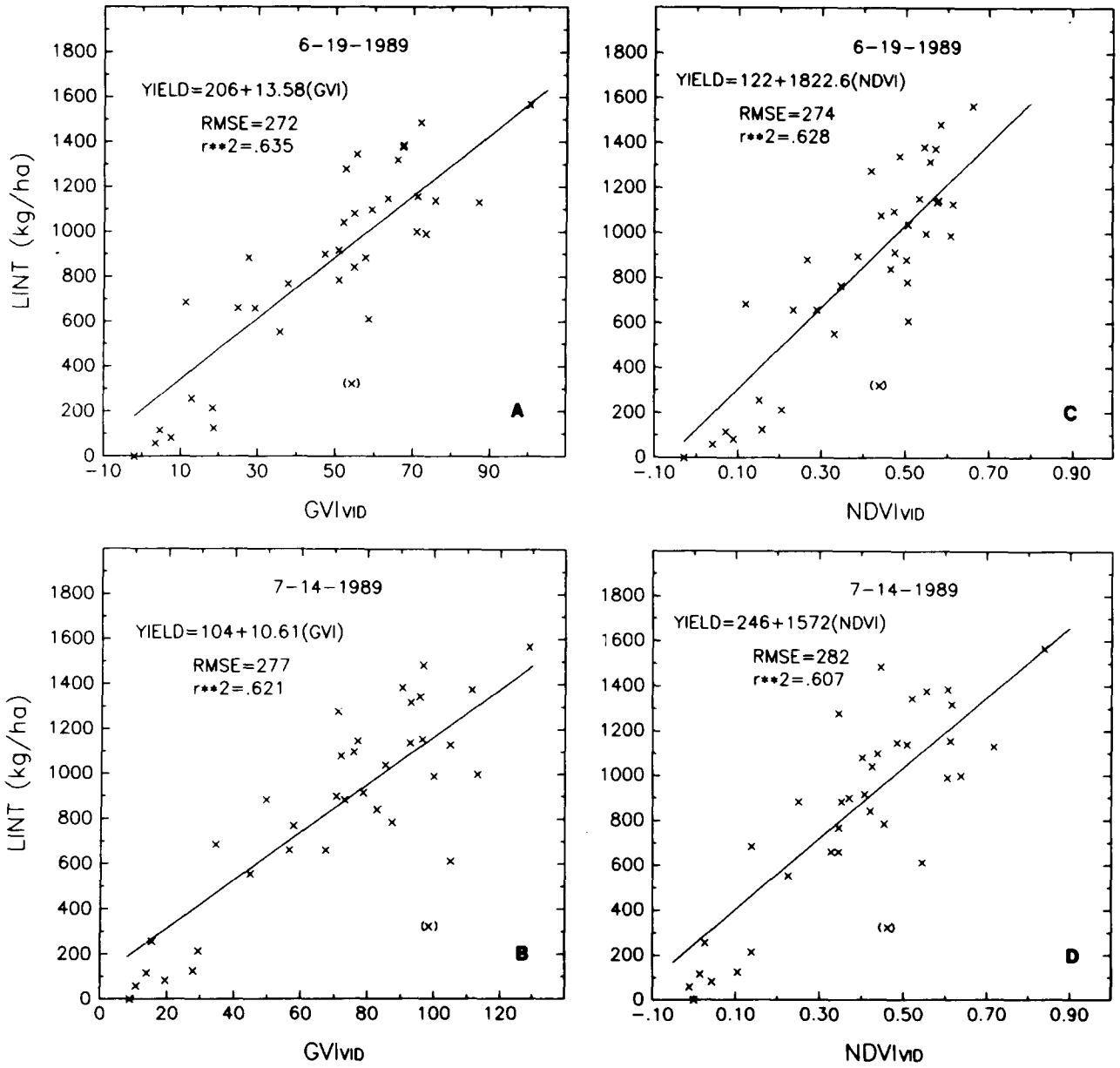

Figure 2. Lint yield of cotton versus GVI and NDVI from multispectral video observations on two dates.

size of the canopy did not change much during the 38 days between the SPOT-1 satellite overpass on 4 June and the boll counts on 12–13 July.

The equations for all the VI are linear and each vegetation index explains 75–76% of the variation in yield. The root mean square error (RMSE) estimate of yield is also either 222 or 223 kg/ha for all VI. Thus they all provide equivalent information. Perpendicular and greenness vegetation indices (PVI, GVI) are both zero for bare soil, making the best fit equations easy to interpret: no lint yield is predicted until GVI and PVI are slightly positive (a few scattered, stunted plants produce some bolls) and lint yield increased by 96 kg/ha and 104 kg/ha per GVI and PVI unit, respectively. The site for one of the samples in Figure 1 was infested with vigorously growing common bermudagrass (*Cynodon dactylon* L.) and this sample, identified by enclosure in parentheses, was left out of the statistical fits.

The relations for percent plant cover at the 36 sampling sites versus the same VI) in Figure 1 (not shown) gave coefficients of determination (r^2) and RMSE (in parentheses) pairs of 0.66 (10%), 0.67 (9%), 0.68 (9%), and 0.68 (9%) for NDVI, TSAVI, PVI, and GVI, respectively.

The lint yield versus GVI and NDVI as in the left side term of Eq. (7) for video data collected on 19 June and 14 July is shown in Figure 2. The coefficients of determination are slightly higher for 19 June than for 14 July, but lower for both dates than for the SPOT-1 HRV data. By 14 July bolls were opening and harvest was only about 3 weeks away. In Figure 2, the GVI are much larger than in Figure 1 because they are based on digital counts that had values about five times as large as the reflectances used for the HRV data. The HRV sensor has a nominal ground resolution of 20 m whereas the 49 video pixels represented a distance 7.2 m across the rows and 9.3 m down the rows.

Corn

Experimental data for the left side of Eq. (7), FPAR as a function of VI, are presented in Figure 3 for two vegetation indices, PVI and NDVI. We did not experimentally determine the right-hand side terms because Eq. (7), itself, implies that it is not necessary to do so. Experimental data in the literature (Gallo et al., 1985; Wiegand and Richardson, 1987) also show that FPAR can be estimated well from VI as Figure 3 demonstrates again ($r^2 = 0.956$ and 0.973 for PVI and NDVI, respectively), during the pretasseling (first tassels became visible on 8 May and the maximum VI readings occurred on 9 May before they had emerged) or pre-VImax period. When the tassels fully emerged, they shaded the sensors measuring transmittance (T) and FPAR increased by 0.10–0.15. Thus PAR was intercepted by photosynthetically inactive tissue (Rosenthal et al., 1985) which perverts FPAR defined by Eq. (1). The solution we have suggested is use of VI measured throughout the season in the functional relation between FPAR and VI developed from the pre-VImax portion of the season.

In Figure 3, the post-VImax regression line and equation are for the data pooled among populations. However, it is known (e.g., Rosenthal et al., 1985) that FPAR for the post-VImax period intercepts the FPAR axis between 0.3 and 0.7 for a completely senescent canopy depending upon density of the stand. Consequently, had experimental FPAR observations continued after 16 June, the low population treatment, at least, would require a different fit from the other two treatments and would likely intercept below 0.3.

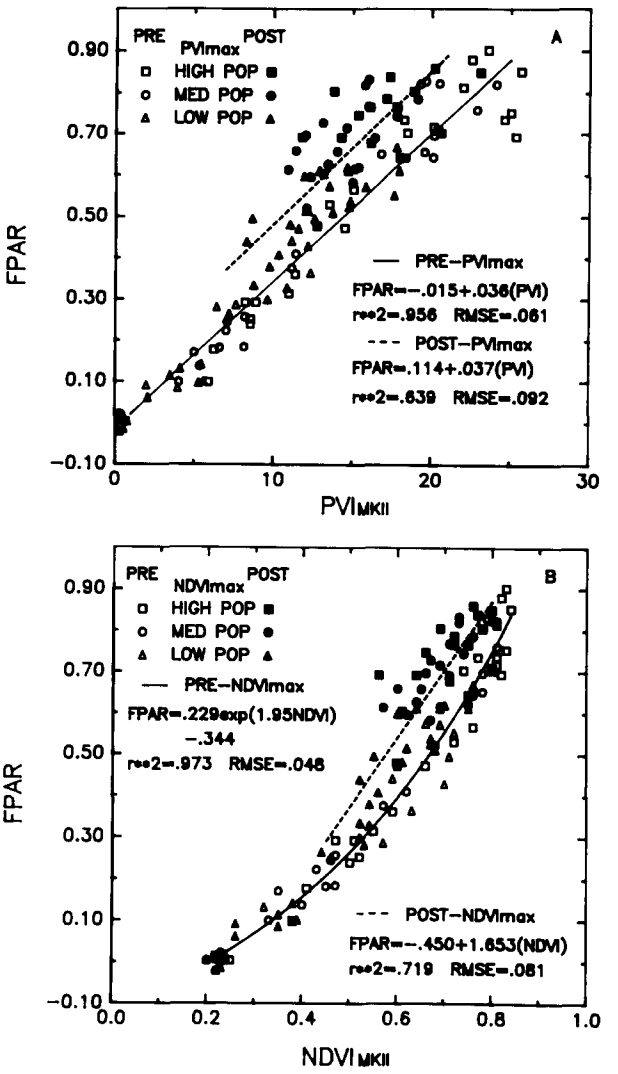

Figure 3. Fractional absorbed PAR, FPAR, as a function of PVI and NDVI for corn by pre-VImax and post-VImax periods.

Figure 4 which displays experimentally observed PVI and FPAR by population treatment versus day of year (DOY) shows that PVI decreased after the tassels emerged whereas FPAR continued at a plateau value for three more observation dates. We have accounted for this discrepancy in discussing Figure 3.

Data for the left hand side of Eq. (7) are presented in Figure 5a for each individual plot for an observation date, 5 June, that was halfway through grain filling, while the seasonal cumulative PVI, corresponding to the left side of Eq. (8) is presented in Figure 5b. The 1-m^2 samples for grain yield were inadequate and contributed to the scatter in Figure 5. The low population treatment

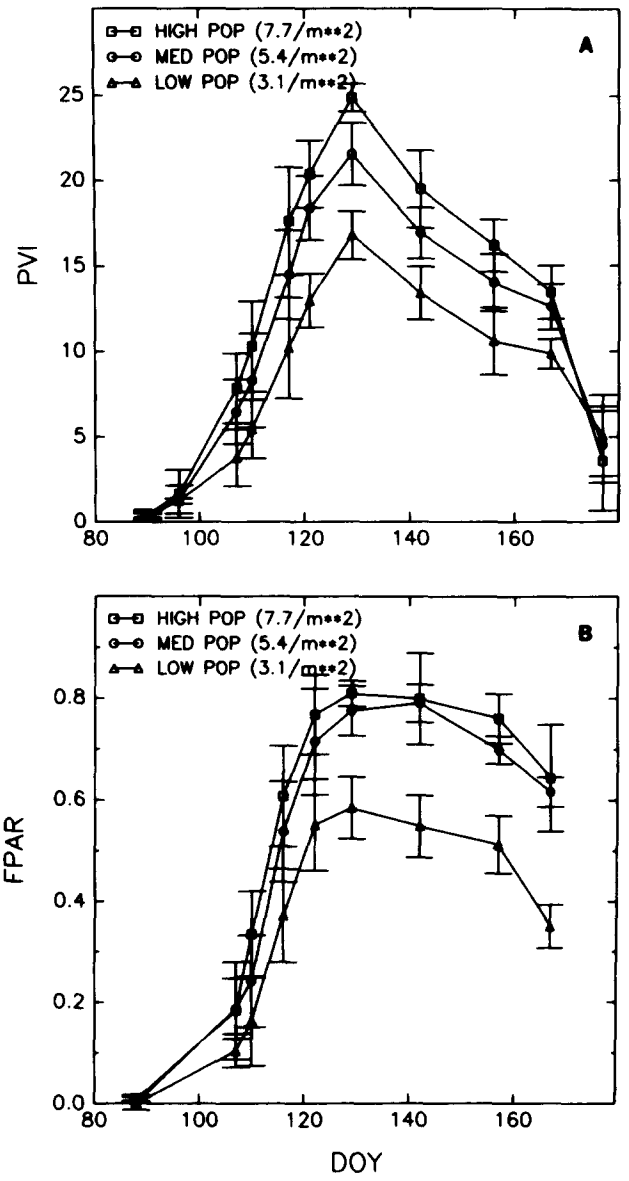

Figure 4. Experimentally observed PVI and FPAR means and standard deviations by population treatment versus day of year (DOY) for corn.

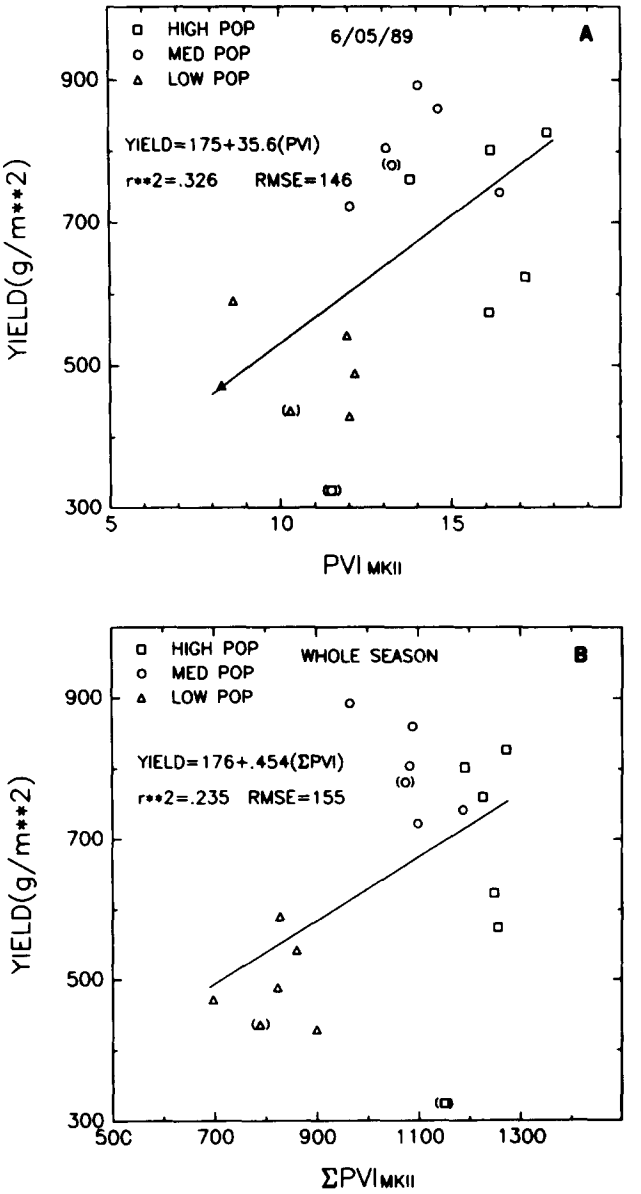

Figure 5. Grain yield of corn versus PVI on one date [left side of Eq. (7)] and cumulative PVI for the growing season, ΣPVI [left side of Eq. (8)].

had too few plants/m^2 to utilize the PAR effectively (Fig. 4) and there was insufficient elasticity in ear size to compensate for the deficit in plant population. The medium population was about that recommended locally for commercial corn production and there was a good balance among plant population, fertility, water, and available PAR resources. There were too many plants in the high population for the nutrient conditions that existed and very small ears were produced that yielded less grain/m^2 than did the medium population. The data point enclosed in parentheses for one plot of each treatment is from the first tier of plots on one side of the experimental area where the plants were visibly nitrogen deficient due to leaching by excessive irrigation the previous crop season.

The data of Figure 5 illustrate that interpretation is aided by agronomic understanding of limiting factors in crop growth and yield (often revealed through the patterns seen in multitemporal imagery of the ground scenes). The approach is intended to apply to commercial crops husbanded by recommended practices for the production area where grown.

Table 2. Solution of Eq. (8) Term by Term for the Whole Corn Growing Season (Emergence to Physiological Maturity of the Grain) by Population Treatment

Population (*plants* / m^2)	$\frac{Yield}{\Sigma PVI}$ ($g\ m^{-2}$ / *PVI unit*)[a]	$= \frac{Yield}{\Delta DM}$ ($g\ m^{-2}$ / $g\ m^{-2}$)[b]	$\times \frac{\Delta DM}{\Sigma APAR}$ (*g* / *MJ*)[c]	$\times \frac{\Sigma APAR}{\Sigma PVI}$ (*MJ* m^{-2} / *PVI unit*)[d]
A. PVI and APAR Summed Daily (based on Fig. 5)				
7.7	0.576	0.436	2.726	0.484
5.4	0.738	0.473	3.000	0.520
3.1	0.611	0.452	2.774	0.487
B. FPAR after 9 May (tasseling) from FPAR = −0.015 + 0.036 (PVI) of Fig. 4a				
7.7	same	same	3.249	0.406
5.4	same	same	3.706	0.419
3.1	same	same	3.251	0.416

[a] Yield efficiency e_y in terms of cumulative perpendicular vegetation index.
[b] Harvest index, HI.
[c] Efficiency of conversion of absorbed PAR to dry matter, e_c.
[d] Efficiency of absorption, e_a, in terms of perpendicular vegetation index.

The solution of Eq. (8) for the whole corn growing season (emergence to physiological maturity of the grain) is presented term by term by population treatment in Table 2. Absorbed PAR was calculated two ways: 1) by multiplying experimental FPAR of Figure 4b by the unique observed daily incident PAR flux (upper part of Table 2), and 2) as in 1), above, through 9 May but thereafter by inserting observed daily values of PVI into the pre-PVImax (pretasseling) FPAR equation in Figure 3a and multiplying that answer by the incident PAR flux for each day. Cumulative (or integral) APAR was obtained by summing the daily values throughout the season.

This procedural difference affects the last two right side terms of Eq. (8), the efficiency of conversion of absorbed PAR to dry matter, e_c, and the efficiency of absorption in terms of the vegetation index, e_a. Since ΣAPAR is smaller when photosynthetically inactive tissue affecting FPAR is minimized, e_c is 1.19, 1.24, and 1.17 times larger for high, medium, and low plant populations, respectively, in the lower than in the upper part of Table 2. The values in the lower part of Table 2 agree well with the value of 3.4 g DM/MJ PAR recommended for corn by Sinclair and Horie (1989). Likewise, the efficiencies of absorption are smaller by almost these same factors. We conclude that work needs to be done to educate users about the variability in efficiencies of conversion of PAR to dry matter based on methods of determining FPAR.

In Table 2, the harvest indices—the slope of grain yield as a function of total aboveground dry matter including the grain—ranged from 0.436 for the densest population to 0.473 for the intermediate planting. This range is quite narrow but still important. At harvest total above ground air-dry phytomass, DM_2, was 1645, 1700, and 1115 g/m^2 for high, medium, and low populations, respectively. For $DM_2 = 1500$, each 0.01 increase in the harvest index means a 15 g/m^2 or 150 kg/ha increase in grain yield, enough to make a difference in profit or loss to the grower in current narrow profit–loss margins.

The yield efficiency, the left side term in Eq. (8) was in the same order as the efficiency of absorption, the same finding reported by Wiegand et al. (1989) for rice. In that study there were 13 treatments consisting of incomplete combinations of two planting dates, three cultivars, and 6N application rates. Relative to the mean, variation in the ΣAPAR(ΣPVI) term was about 15% compared with 5% for the other two right side terms, so that it dominated the Y(ΣPVI) term. It is not necessary to know which of the right side terms in Eq. (8) determine ΣVI for it to become a viable remote estimator of yield. That is highly desirable for scientific understanding and can be established by additional intensive small plot studies.

DISCUSSION

The spectral components analysis (SCA) equations reviewed and illustrated provide a framework within which to examine a large number of relationships that describe the growth, photosynthetic

size, and yield of crops as affected by their environments and stresses. The spectral terms (those involving VI) interrelate VI, L, FPAR, APAR, yield, and DM in a way that is consistent with physical and physiological principles and in agreement with growth and yield behavior of crops in the field. Internal consistency is enhanced by the facts that FPAR, VI, and yield all approach limiting values asymptotically as L increases (Wiegand and Richardson, 1984; Sellers, 1985).

The equations were developed to maximize the information extractable from spectral observations about crop conditions and yields. The left side terms of Eqs. (6), (7), and (8) are emphasized to take advantage of remote observation capability while the right sides address the plant processes involved. Until the equations were developed, there was no theory to undergird the interpretations. Hopefully, SCA will increase the appeal of spectral observations to other potential users of this capability, for example, plant process modelers, ecologists, hydrologists, and meteorologists.

Satellite observation capability should permit estimation of FPAR for vegetated areas expressed by

$$\text{FPAR} = (1 - R)(1 - T), \qquad (10)$$

wherein surface reflectance R can be approximated by a broad visible band such as the panchromatic band (510–730 nm) of the SPOT-1 HRV. One limit of R is the reflectance of bare soil (0.05–0.20, depending on water content and color) and the other extreme is the infinite reflectance of the canopy (0.03–0.05). Intercepted PAR, $(1 - T)$, can be estimated by the SAIL or other canopy reflectance model from observed NIR and RED band reflectances. If capability to execute the SAIL model is lacking, the functional relation between $(1 - T)$ and VI may be found in the literature or can be experimentally developed for the crop(s) of interest. Since $[I_0(1 - R)]$ is also physically the net downward flux, APAR ($MJ/m^2/day$) is the product $[I_0(1 - R)](1 - T)$. For bare soil $T = 1.0$ so that APAR = 0, and for a very dense canopy T approaches 0, so that APAR = $(0.95–0.97)I_0$. Periodic remote observations of R and model estimates of T near solar noon permit graphs of $(1 - R)$ and $(1 - T)$ versus DOY (like Fig. 4) from which estimates for all days of interest can be made. Choudhury (1987) has used a radiative transfer equation to estimate FPAR and Baret and co-workers (e.g., Baret and Olioso, 1989) have used the SAIL model in conjunction with estimates of light absorption by canopies but not in context of Eq. (10). Advances must be made in standardizing the estimation of PAR absorption by canopies, lest the efficiencies of conversion of APAR to DM will remain variable. In this study the two methods of calculation used gave values that differed by about 20%.

It is evident that ΣVI is similar in some respects to leaf area duration (LAD) proposed by Watson (1952), which has largely been abandoned because it did not hold across environments (Evans and Wardlaw, 1976). (LAD used here is not to be confused with leaf angle distribution as used in canopy radiative transfer modeling.) Leaf area duration had the units, days, and made no distinction between, for example, cool, low irradiance winter and warm, high irradiance summer days. In contrast, the VI measure the photosynthetic size of the canopies as affected by environmental variables. The variables that control the potential VI are stable for a given production area from year to year (daylength or insolation, inherent soil properties, cultivars, management practices) while the stress variables (precipitation, diseases, toxic pesticide residues, weather events, etc.) are growing-season-dependent. Therefore, calibrations of yield versus VI across good and poor growing conditions within production areas can describe the results of past and future growing seasons acceptably.

The calibrations are needed presently because two of the three right side terms in Eq. (8) are site-dependent. We speculate that the dominant environmental variable causing variability in the ΔDM(ΣAPAR) functional relation is ambient temperature; in principle, any stress such as low temperature to which cell expansion and photosynthesis differ in sensitivity, or above optimum temperature within the plant tolerance range to which respiration and photosynthesis differ in sensitivity, can cause deviation from constancy in the efficiency of conversion.

The harvest index is highest for a given crop where it is best adapted and decreases as it is grown under less ideal conditions. We speculate that saturation deficits of the air, insolation, and air and soil temperatures that are partly controlled by latitude and elevation are probably the important

factors. Unfortunately, the factors that cause the efficiency of conversion and the harvest index to vary geographically are poorly researched.

In terms of applying Eqs. (7) and (8), we can say that the left side terms would not be site-dependent if the right side terms were not. Likewise, if the right side site dependencies were known, the left side site dependencies would be predictable and the left side functional relations would not have to be calibrated by production areas. On the other hand, if the left side term functional relations are carefully determined, they can help elucidate the right side functional relations.

In summary, observed yield differences among fields are associated with differences in L, DM, and percent cover that start becoming evident in the vegetation indices early in vegetative development (e.g., Richardson et al., 1982). The differences in growth have many possible causes (management practices, weather, inherent soil properties, biotic stresses, etc.). Direct observation of the photosynthetic size of the canopies and the interpretation of those observations within the framework of spectral components analysis permits inferences about the development, growth, and yield of the plant communities that constitute the canopies observed. Yield was emphasized in the paper because of its economic importance to producers and in world trade.

We thank Dr. Melba Crawford, University of Texas, Austin, for providing the SPOT-1 scene; Dr. Stephan Maas for designing the corn experiment and getting it initiated; Edgar Smith for allowing us to use his cotton field; Rene Davis for piloting the plane to acquire the video data and for printing Plate I; Noel Garcia for processing data on the image analysis systems; Romeo Rodriguez and Alvin Gerbermann for assistance with field work, data reduction, statistical analysis, and for figure preparation; and Carol Harville and Saida Cardoza for manuscript preparation.

REFERENCES

Aase, J. K., and Siddoway, F. H. (1981), Spring wheat yield estimates from spectral reflectance measurements, *IEEE Trans. Geosci. Remote Sens.* 19:78–84.

Baret, F., and Olioso, A. (1989), Estimation à partir de mesures de rèflectance spectrale du rayonnement photosynthètiquement actif absorbè par une culture de blè, *Agronomie* 9:885–895.

Baret, F., Guyot, G., and Major, D. J. (1989), TSAVI: A vegetation index which minimizes soil brightness effects on LAI and APAR estimation, in *Proc. IGARSS '89—12th Canadian Symp. on Remote Sens.* 3:1355–1358.

Carter, D. L., and Wiegand, C. L. (1965), Interspersed salt-affected and unaffected dryland soils of the Lower Rio Grande Valley: I. Chemical, physical, and mineralogical characteristics, *Soil Sci.* 99:256–260.

Choudhury, B. J. (1987), Relationship between vegetation indices, radiation absorption, and net photosynthesis evaluated by sensitivity analysis, *Remote Sens. Environ.* 22:209–233.

Curran, P. (1980), Multispectral sensing of vegetation amount, *Prog. Phys. Geog.* 4:315–341.

Evans, L. C. and Wardlaw, I. F. (1976), Aspects of comparative physiology of grain yield in cereals, *Adv. Agron.* 28:301–350.

Everitt, J. H., Escobar, D. E., Villarreal, R., Noriega, J. R., and Davis, M. R. (1991), Airborne video systems for agricultural assessment, presented at BARC Symp., Greenbelt, MD, 16–18 May 1990, *Remote Sens. Environ.* 34:233–244.

Gallo, K. P., Daughtry, C. S. T., and Bauer, M. E. (1985), Spectral estimation of absorbed photosynthetically active radiation in corn canopies, *Remote Sens. Environ.* 17:221–232.

Goel, N. S. (1988), Models of vegetation canopy reflectance and their use in estimation of biophysical parameters from reflectance data, *Remote Sens. Rev.* 4:1–212.

Goel, N. S., and Thompson, R. L. (1984), Inversion of vegetation canopy reflectance models for estimating agronomic variables. III. Estimation using only canopy reflectance data as illustrated by the Suits model, *Remote Sens. Environ.* 15:223–226.

Hipps, L. E., and Kanemasu, E. T. (1983), Assessing the interception of photosynthetically active radiation in winter wheat, *Agric. Meteor.* 28:253–259.

Holben, B. N., Tucker, C. J., and Fan, C. J. (1980), Assessing soybean leaf area and leaf biomass with spectral data, *Photogramm. Eng. Remote Sens.* 26:651–656.

Howell, T. A. (1990), Grain-dry matter yield relationships for winter wheat and grain sorghum, Southern High Plains, *Agron. J.* 82:914–918.

Jackson, R. D. (1983), Spectral indices in n-space, *Remote Sens. Environ.* 13:409–421.

Jackson, R. D., Pinter, P. J., Jr., Reginato, R. J., and Idso, S. B. (1980), Hand-held radiometry, USDA-SEA, Agric. Rev. and Manuals, ARM-W-19, 66 pp.

Kauth, R. J., and Thomas, G. S. (1976), The tasseled cap—A graphic description of the spectral temporal development of agricultural crops as seen by LANDSAT, in *Proc. Symp. Machine Proc. Remotely Sensed Data*, IEEE, New York, pp. 41–49.

Kimes, D. S., Markham, B. L. and Tucker, C. J. (1981), Temporal relationships between spectral response and agronomic variables of a corn canopy, *Remote Sens. Environ.* 11:401–411.

Monteith, J. L. (1977), Climate and the efficiency of crop production in Britain, *Phil. Trans. Roy. Soc. London B* 281:277–294.

Moran, M. S., Jackson, R. D., Hart, G. F., Slater, P. N., Bartell, R. J., Biggar, S. F., Gellman, D. I., and Santer, R. P. (1990), Obtaining surface reflectance factors from atmospheric and view angle corrected SPOT-1 HRV data, *Remote Sens. Environ.* 32:203–214.

Pearson, R. L., Miller, L. D., and Tucker, C. J. (1976), Handheld spectral radiometer to estimate graminous biomass, *Appl. Opt.* 15:416–418.

Perry, C. A., Jr., and Lautenschlager, L. P. (1984), Functional equivalence of spectral vegetation indices, *Remote Sens. Environ.* 14:169–182.

Pinter, P. J., Jr., Jackson, R. D., Idso, S. B., and Reginato, R. J. (1981), Multidate spectral reflectance as predictors of yield in water stressed wheat and barley, *Int. J. Remote Sens.* 2:43–48.

Richardson, A. J. (1981), Measurement of reflectance factors under daily and intermittent irradiance variations, *App. Opt.* 20:3336–3340.

Richardson, A. J., and Wiegand, C. L. (1977), Distinguishing vegetation from soil background information, *Photogramm. Eng.* 43:1541–1552.

Richardson, A. J., Gautreaux, M. R., Torline, R. J., and Wiegand, C. L. (1974), Land use classification and ground truth correlations from simultaneously acquired aircraft and ERTS-1 MSS data, in *Proc. Ninth Int. Symp. on Remote Sens. Environ.* Univ. of Michigan, Ann Arbor, Vol. II, pp. 1423–1440.

Richardson, A. J., Wiegand, C. L., Arkin, G. F., Nixon, P. R., and Gerbermann, A. H. (1982), Remotely sensed spectral indicators of sorghum development and their use in growth modeling, *Agric. Meteorol.* 26:11–23.

Rosenthal, W. D., Arkin, G. F., and Howell, T. A. (1985), Transmitted and absorbed photosynthetically active radiation in grain sorghum. *Agron. J.* 77:841–845.

Rouse, J. W., Jr., Haas, R. H., Schell, J. A., and Deering, D. W. (1973), Monitoring vegetation systems in the Great Plains with ERTS, in *Third ERTS Symp.*, NASA SP-351, U.S. Gov. Printing Office, Washington, DC, Vol. I, pp. 309–317.

Sellers, P. J. (1985), Canopy reflectance, photosynthesis and transpiration, *Int. J. Remote Sens.* 6:1335–1372.

Sellers, P. J. (1987), Canopy reflectance, photosynthesis, and transpiration. II. The role of biophysics in the linearity of their interdependence, *Remote Sens. Environ.* 21:143–183.

Sinclair, T. R., and Horie, T. (1989), Leaf nitrogen, photosynthesis, and crop radiation use efficiency: a review, *Crop Sci.* 29:90–98.

SPOT User's Handbook, Rev. 01 (1989), Vol. 1, Reference Manual, SPOT Image Corporation, Reston, VA.

Thomas, J. R., and Gausman, H. W. (1977), Leaf reflectance vs. leaf chlorophyll and carotenoid concentrations for eight crops, *Agron. J.* 69:799–802.

Tucker, C. J. (1977), Spectral estimation of grass canopy variables, *Remote Sens. Environ.* 6:11–16.

Tucker, C. J. (1979), Red and photographic infrared linear combinations for monitoring vegetation, *Remote Sens. Environ.* 8:127–150.

Tucker, C. J., Elgin, J. H., Jr., McMurtrey, J. E., III, and Fan, C. J. (1979), Monitoring corn and soybean crop development with hand-held radiometer spectral data, *Remote Sens. Environ.* 13:461–474.

Tucker, C. J., Jones, W. H., Kley, W. A., and Sundstrom, G. T. (1981), A three-band hand-held radiometer for field use, *Science* 211:281–283.

Tucker, C. J., Vanpraet, C., Boerwinkel, E., and Gaston, A. (1983), Satellite remote sensing of total dry matter production in the Senegalese Sahel, *Remote Sens. Environ.* 13:461–474.

Tucker, C. J., Townshend, J. R. G., and Goff, T. E. (1985), African land-cover classification using satellite data, *Science* 227:369–375.

Verhoef, W. (1984), Light scattering by leaf layers with application to canopy reflectance modeling: the SAIL model, *Remote Sens. Environ.* 16:125–141.

Walburg, G., Bauer, M. E., Daughtry, C. S. T., and Housley, T. L. (1982), Effects of nitrogen nutrition on the growth, yield, and reflectance characteristics of corn canopies, *Agron. J.* 74:677–683.

Warren Wilson, J. (1981), Analysis of growth, photosynthesis and light interception for single plants and stands, *Ann. Bot.* 48:507–512.

Watson, D. J. (1952), The physiological basis of variation in yield, *Adv. Agron.* 4:101–146.

Wiegand, C. L., and Richardson, A. J. (1984), Leaf area, light interception, and yield estimates from spectral components analysis, *Agron. J.* 76:543–548.

Wiegand, C. L., and Richardson, A. J. (1987), Spectral components analysis. Rationale, and results for three crops, *Int. J. Remote Sens.* 8:1011–1032.

Wiegand, C. L., and Richardson, A. J. (1990), Use of spectral vegetation indices to infer leaf area, evapotranspiration and yield: I. Rationale, *Agron. J.* 82:623–629.

Wiegand, C. L., Gausman, H. W., Cuellar, A. J., Gerbermann, A. H., and Richardson, A. J. (1973), Vegetation density as deduced from ERTS-1 MSS response, in *Third ERTS Symp.*, NASA SP-351, U.S. Gov. Printing Office, Washington, DC, Vol. I, pp. 93–116.

Wiegand, C. L., Richardson, A. J., and Kanemasu, E. T. (1979), Leaf area index estimates for wheat from LANDSAT and their implications for evapotranspiration and crop modeling, *Agron. J.* 71:336–342.

Wiegand, C. L., Richardson, A. J., and Nixon, P. R. (1986a), Spectral components analysis: a bridge between spectral observations and agrometeorological crop models, *IEEE Trans. Goesci. Remote Sens.* GE-24:83–89.

Wiegand, C. L., Richardson, A. J., Jackson, R. D., Pinter, P. J., Jr., Aase, J. K., Smika, D. E., Lautenschlager, L. F., and McMurtrey, J. E., III (1986b), Development of agrometeorolgical crop model inputs from remotely sensed information, *IEEE Trans. Geosci. Remote Sens.* GE-24:90–98.

Wiegand, C., Shibayama, M., Yamagata, Y., and Akiyama, T. (1989), Spectral observations for estimating the growth and yield of rice, *Jpn. J. Crop Sci.* 58:673–683.